

Tetragonal and Trigonal Mo_2B_2 Monolayers: Two New Low-Dimensional Materials for Li-Ion and Na-Ion Batteries

Tao Bo^{a,b}, Peng-Fei Liu^{a,b}, Junrong Zhang^{a,b}, Fangwei Wang^{a,b,c}, Bao-Tian Wang^{a,b,d,*}

^a Institute of High Energy Physics, Chinese Academy of Science (CAS), Beijing 100049, China

^b Dongguan Neutron Science Center, Dongguan 523803, China

^c Beijing National Laboratory for Condensed Matter Physics, Institute of Physics, Chinese Academy of Sciences, Beijing 100080, China

^d Collaborative Innovation Center of Extreme Optics, Shanxi University, Taiyuan, Shanxi 030006, China

E-mail: wangbt@ihep.ac.cn

1. Metastable isomers of 2D Mo_2B_2 .

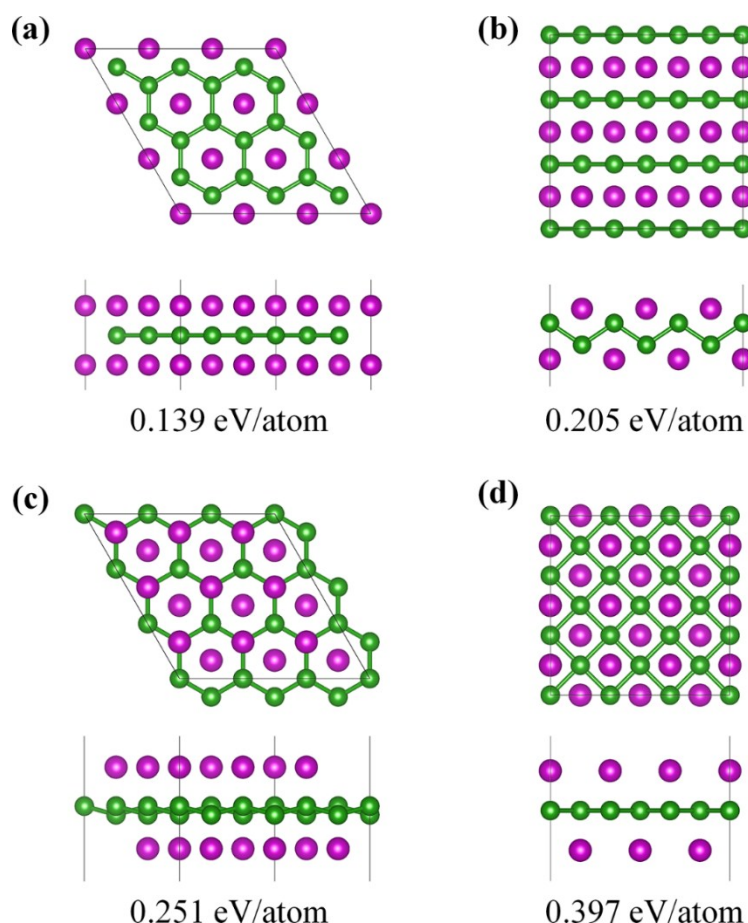


Fig. S1. Metastable isomers of 2D Mo_2B_2 found by the CALYPSO structure search. The Mo and B atoms are denoted by violet and green spheres, respectively.

2. *Ab initio* molecular dynamics (AIMD) analysis of the tetr- Mo_2B_2 and tri- Mo_2B_2 .

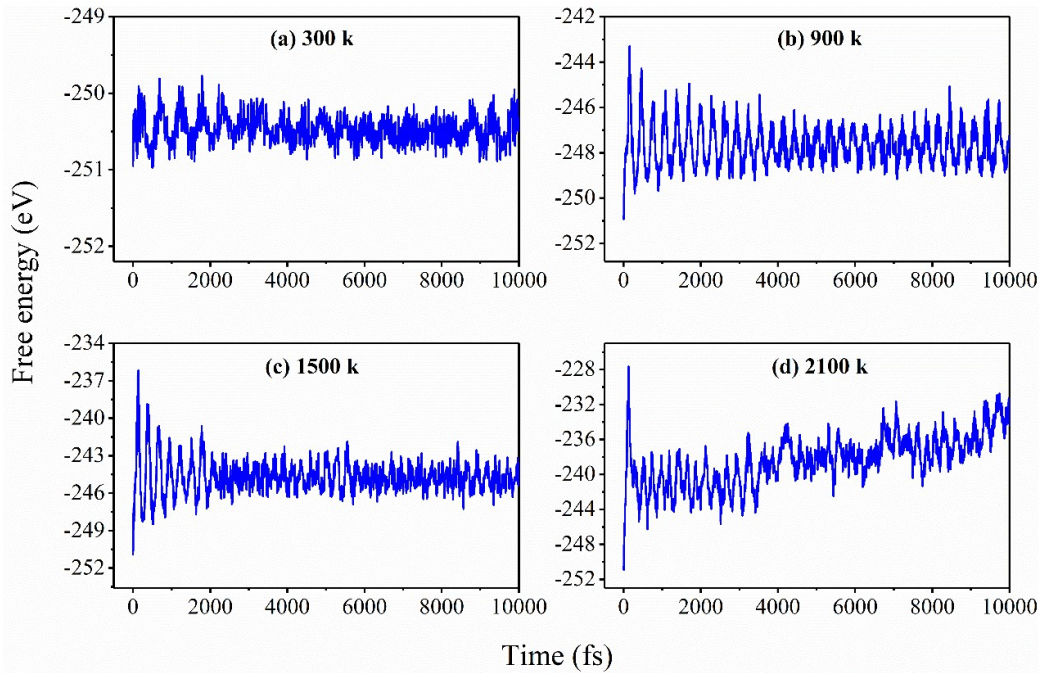


Fig. S2. Variation of the free energy in the AIMD simulations from 300 to 2100 K during the time scale of 10 ps for the tetr- Mo_2B_2 .

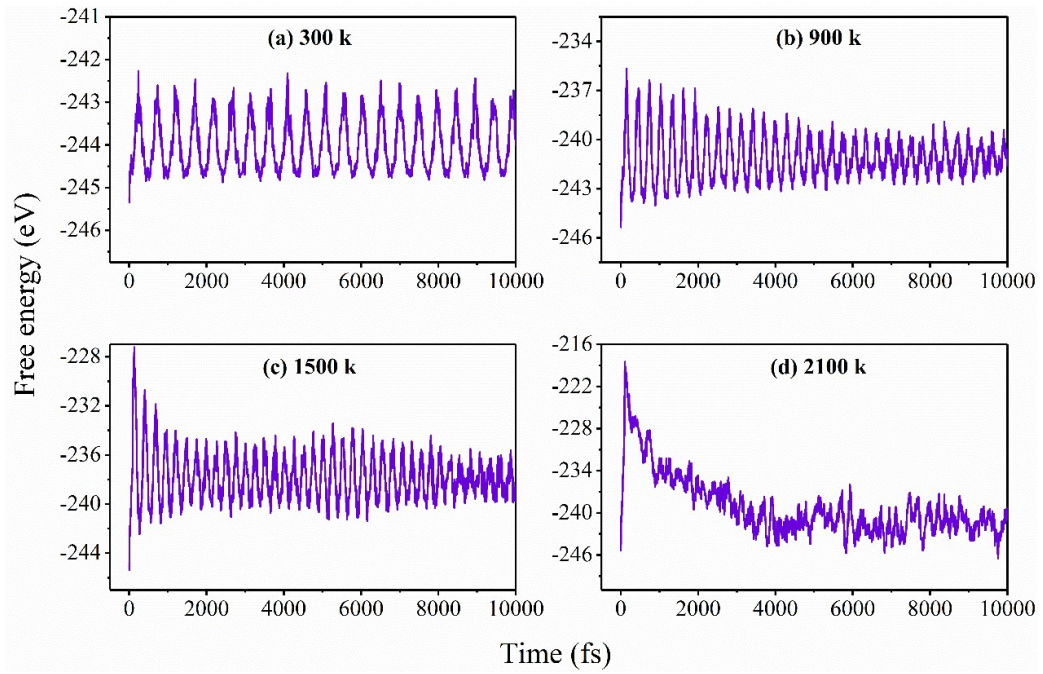


Fig. S3. Variation of the free energy in the AIMD simulations from 300 to 2100 K during the time scale of 10 ps for the tri-Mo₂B₂.

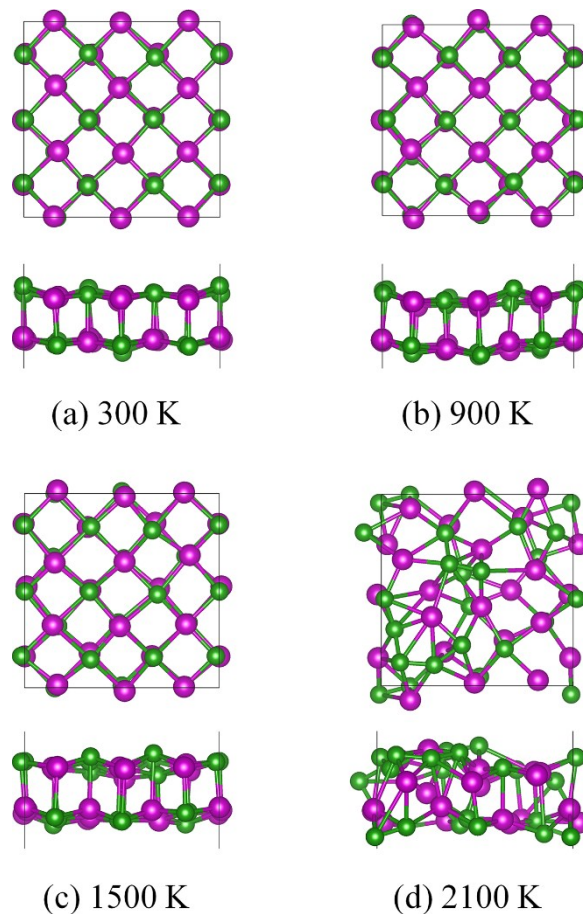


Fig. S4. Snapshots of the tetr-Mo₂B₂ monolayer at temperatures from 300 to 2100 K (top and side views) at the end of 10 ps AIMD simulations. The Mo and B atoms are denoted by violet and green spheres, respectively.

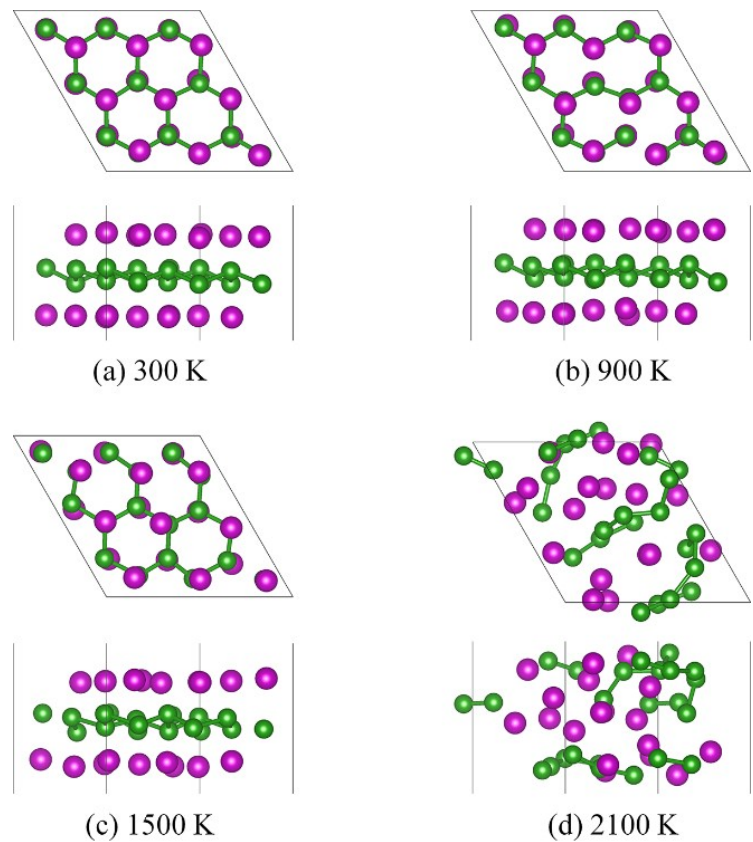


Fig. S5. Snapshots of the tri- Mo_2B_2 monolayer at temperatures from 300 to 2100 K (top and side views) at the end of 10 ps AIMD simulations. The Mo and B atoms are denoted by violet and green spheres, respectively.

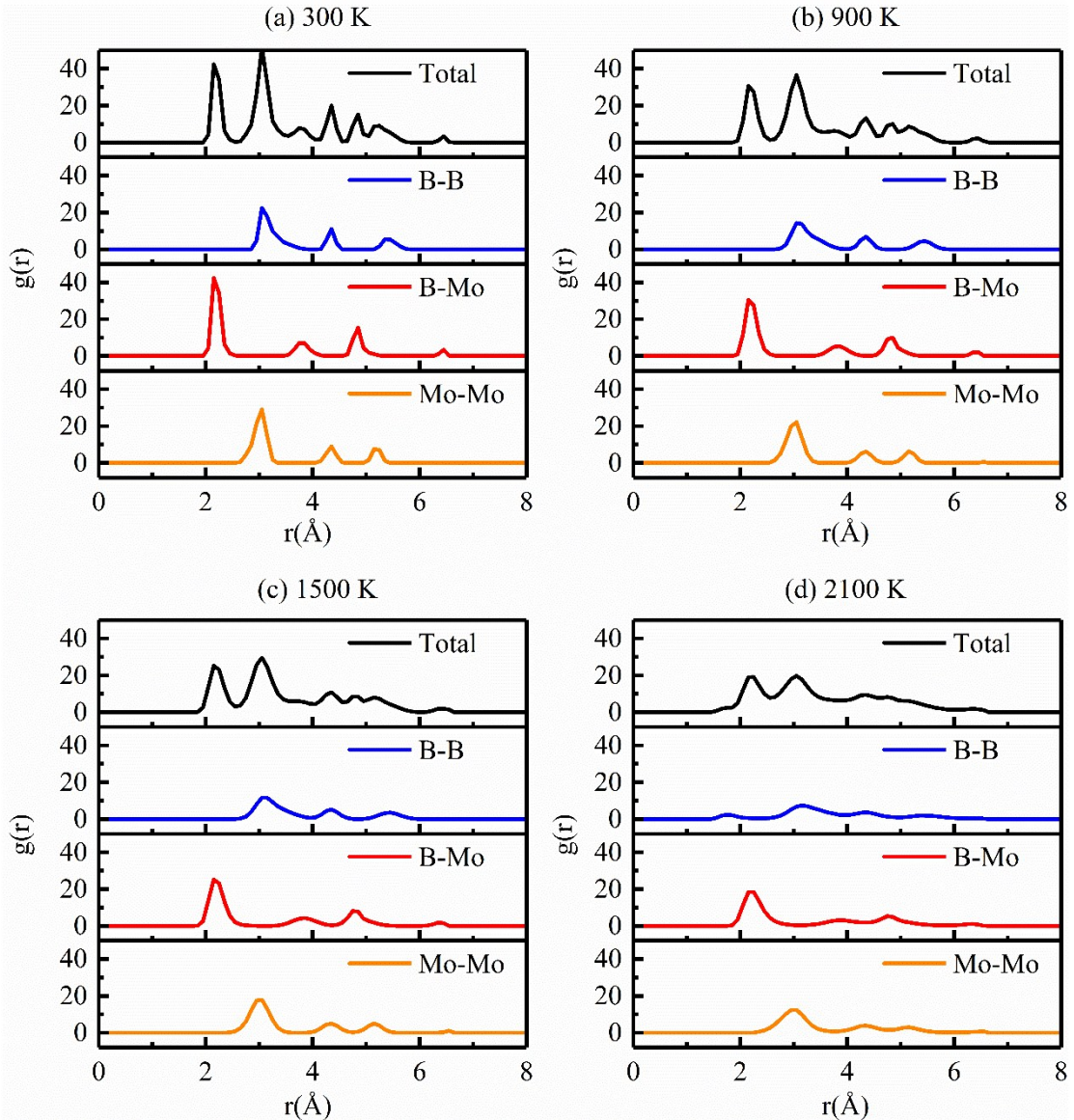


Fig. S6. Radius distribution function (RDF) for the tetr-Mo₂B₂ at (a) 300 K, (b) 900 K, (c) 1500 K, and (d) 2100 K, respectively.

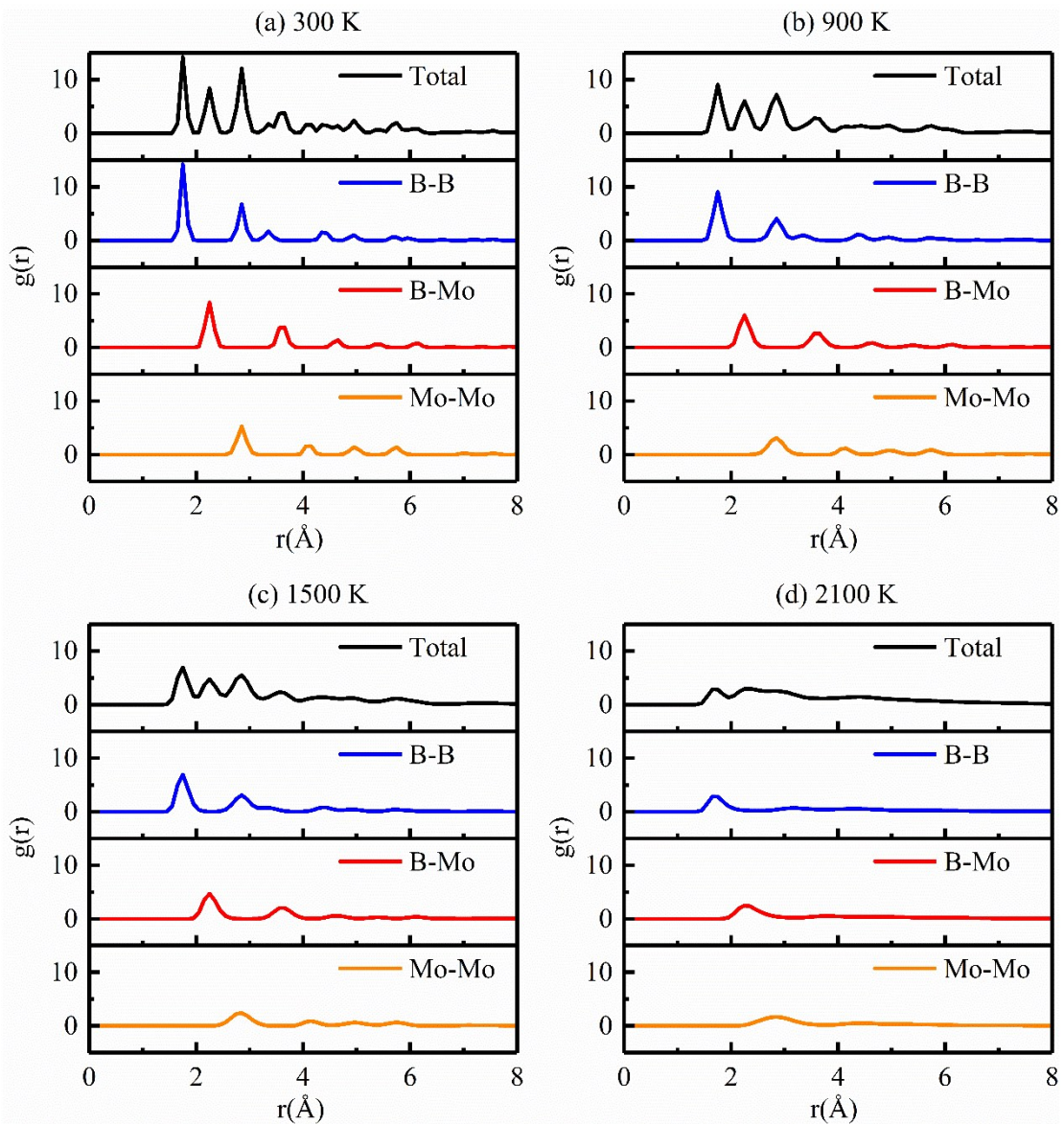


Fig. S7. Radius distribution function (RDF) for the tri- Mo_2B_2 at (a) 300 K, (b) 900 K, (c) 1500 K, and (d) 2100 K, respectively.

3. Adsorption structures and energies of Li/Na with various concentrations on the tetr- Mo_2B_2 and tri- Mo_2B_2

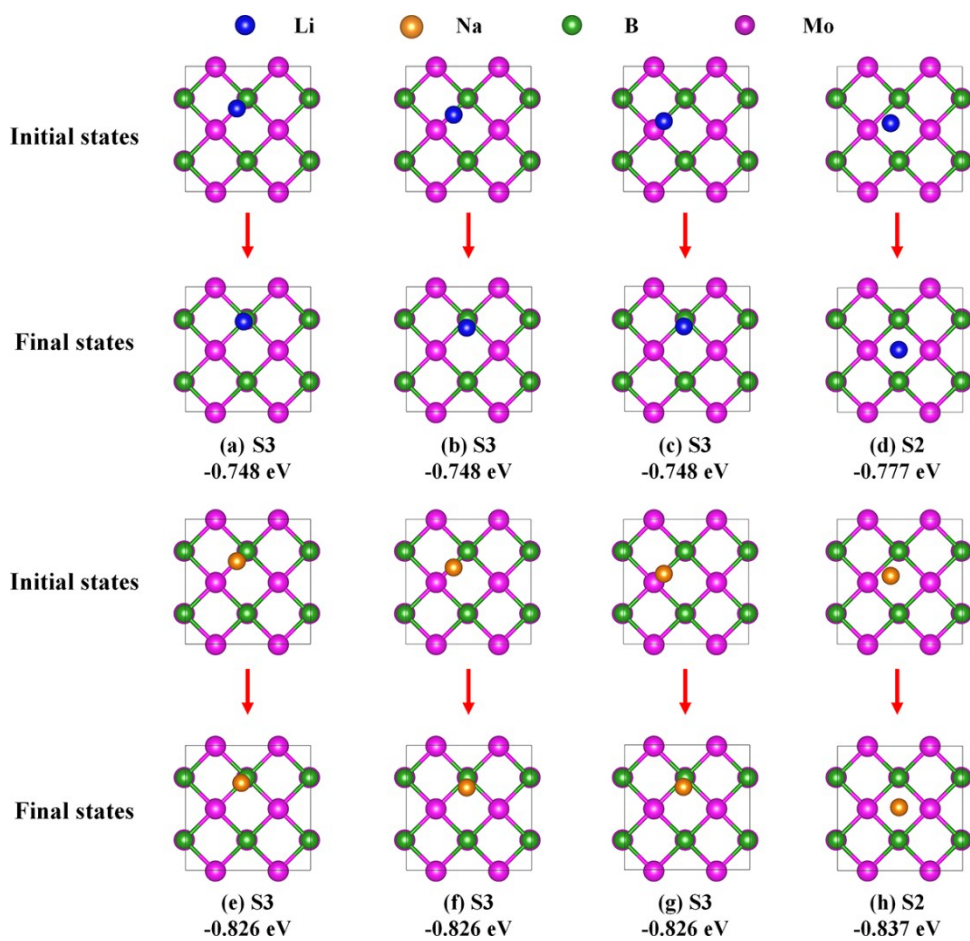


Fig. S8 (a-d) The initial and final states for Li adsorption on different sites of the tetr- Mo_2B_2 . (e-h) The initial and final states for Na adsorption on different sites of the tetr- Mo_2B_2 .

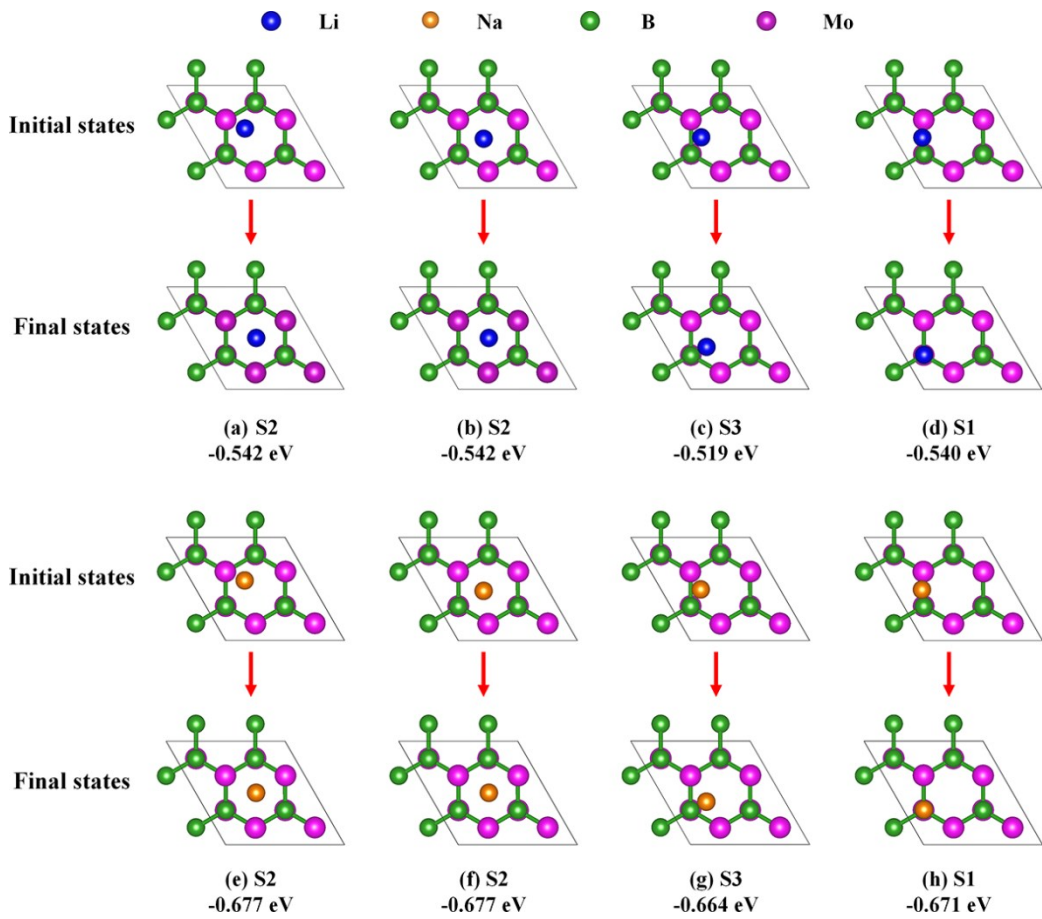


Fig. S9 (a-d) The initial and final states for Li adsorption on different sites of the tri- Mo_2B_2 . (e-h) The initial and final states for Na adsorption on different sites of the tri- Mo_2B_2 .

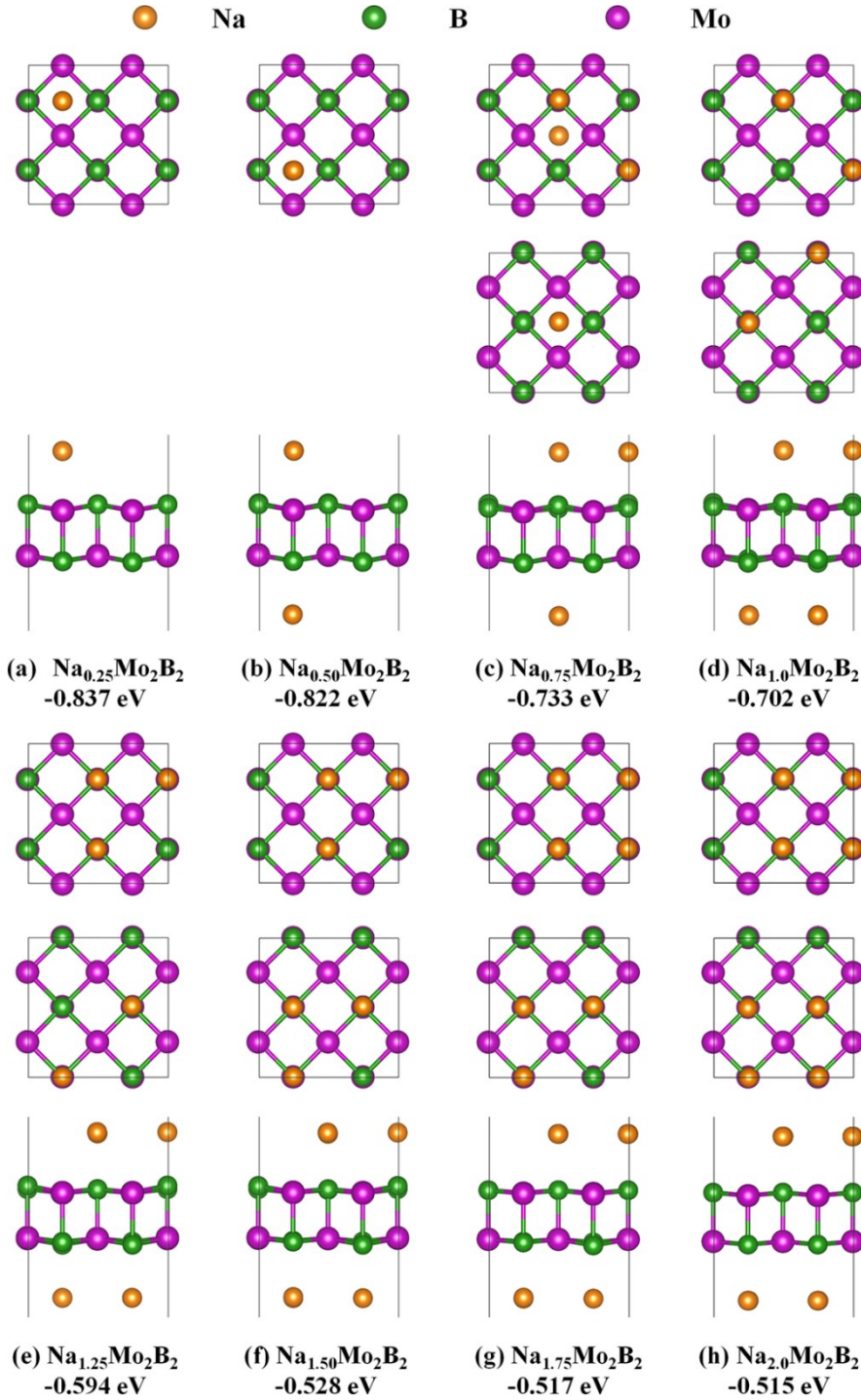


Fig. S10. Top and side views of the structures of (a) $\text{Na}_{0.25}\text{Mo}_2\text{B}_2$, (b) $\text{Na}_{0.50}\text{Mo}_2\text{B}_2$, (c) $\text{Na}_{0.75}\text{Mo}_2\text{B}_2$, (d) $\text{Na}_{1.0}\text{Mo}_2\text{B}_2$, (e) $\text{Na}_{1.25}\text{Mo}_2\text{B}_2$, (f) $\text{Na}_{1.50}\text{Mo}_2\text{B}_2$, (g) $\text{Na}_{1.75}\text{Mo}_2\text{B}_2$, and (h) $\text{Na}_{2.0}\text{Mo}_2\text{B}_2$ with Na ions adsorbed on the surface of the tetr- Mo_2B_2 monolayer. The Mo, B, and Na atoms are denoted by violet, green, and orange spheres, respectively.

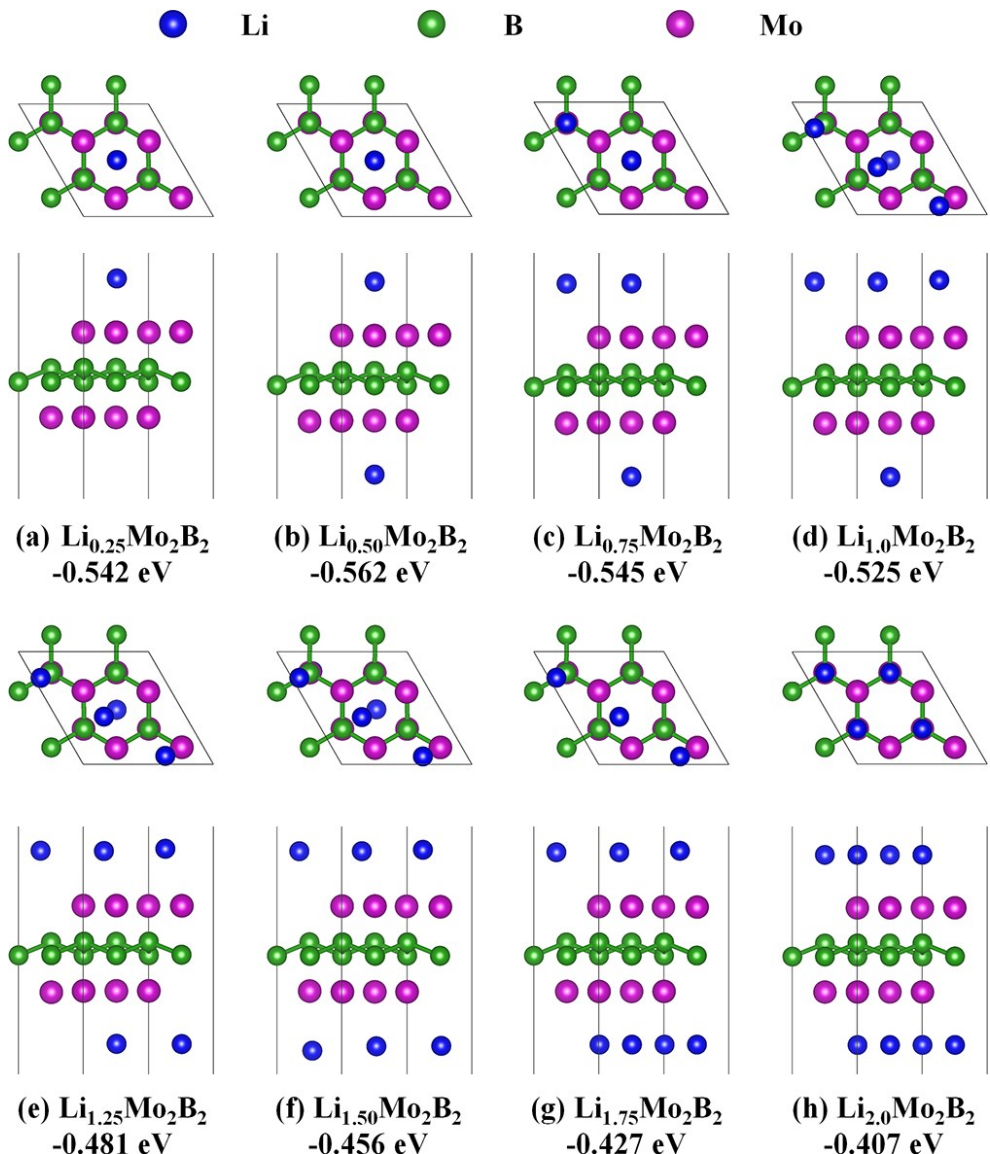


Fig. S11. Top and side views of the structures of (a) $\text{Li}_{0.25}\text{Mo}_2\text{B}_2$, (b) $\text{Li}_{0.50}\text{Mo}_2\text{B}_2$, (c) $\text{Li}_{0.75}\text{Mo}_2\text{B}_2$, (d) $\text{Li}_{1.0}\text{Mo}_2\text{B}_2$, (e) $\text{Li}_{1.25}\text{Mo}_2\text{B}_2$, (f) $\text{Li}_{1.50}\text{Mo}_2\text{B}_2$, (g) $\text{Li}_{1.75}\text{Mo}_2\text{B}_2$, and (h) $\text{Li}_{2.0}\text{Mo}_2\text{B}_2$ with Li ions adsorbed on the surface of the tri- Mo_2B_2 monolayer. The Mo, B, and Li atoms are denoted by violet, green, and blue spheres, respectively.

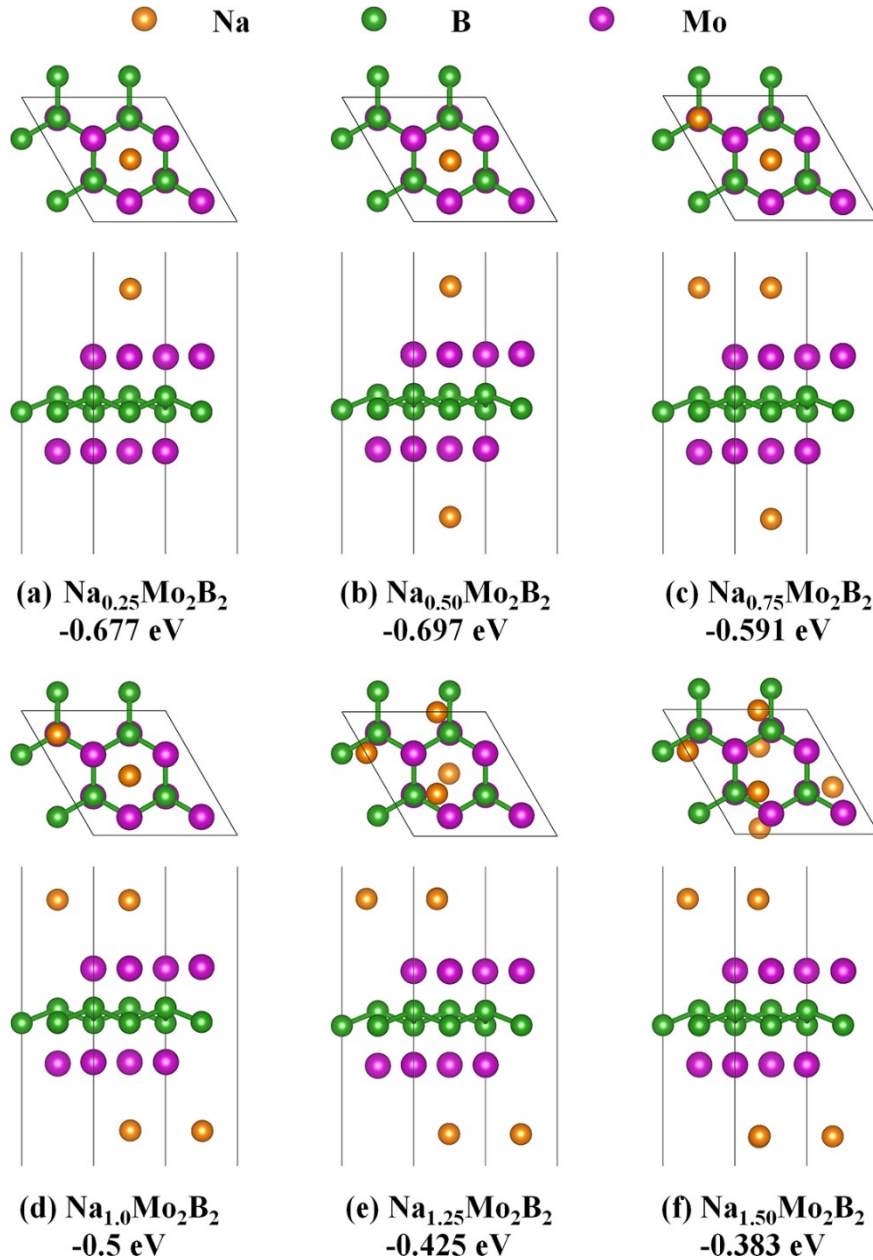


Fig. S12. Top and side views of the structures of (a) $\text{Na}_{0.25}\text{Mo}_2\text{B}_2$, (b) $\text{Na}_{0.50}\text{Mo}_2\text{B}_2$, (c) $\text{Na}_{0.75}\text{Mo}_2\text{B}_2$, (d) $\text{Na}_{1.0}\text{Mo}_2\text{B}_2$, (e) $\text{Na}_{1.25}\text{Mo}_2\text{B}_2$, and (f) $\text{Na}_{1.50}\text{Mo}_2\text{B}_2$ with Na ions adsorbed on the surface of the tri- Mo_2B_2 monolayer. The Mo, B, and Na atoms are denoted by violet, green, and orange spheres, respectively.

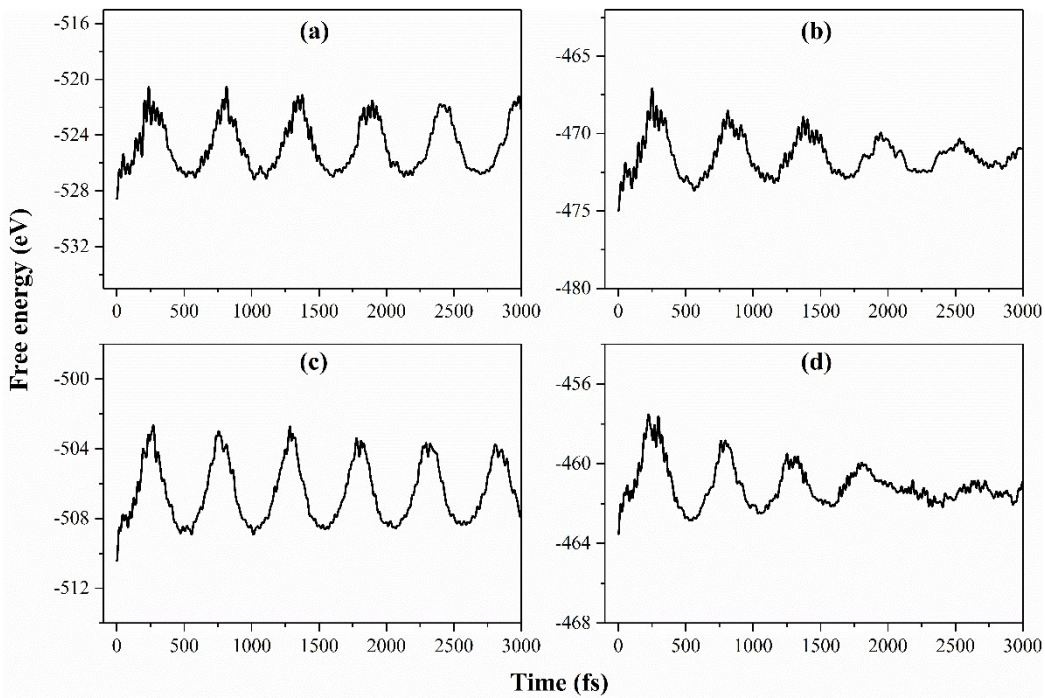


Fig. S13 Variation of the free energies in the AIMD simulations at 300 K during the time scale of 3 ps for the (a) Li adsorbed tetr- Mo_2B_2 , (b) Na adsorbed tetr- Mo_2B_2 , (c) Li adsorbed tri- Mo_2B_2 , and (d) Na adsorbed tri- Mo_2B_2 .

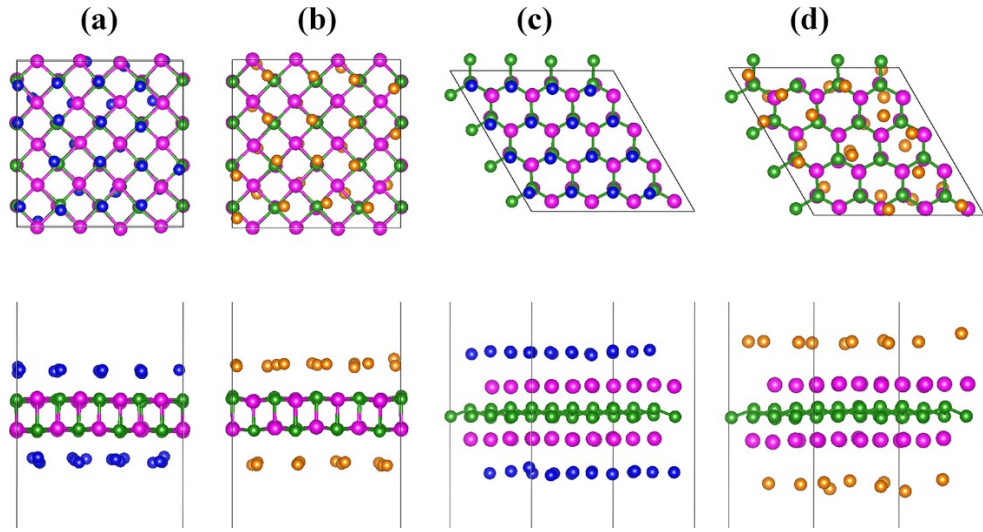


Fig. S14 Snapshots of the (a) Li adsorbed tetr- Mo_2B_2 , (b) Na adsorbed tetr- Mo_2B_2 , (c) Li adsorbed tri- Mo_2B_2 , and (d) Na adsorbed tri- Mo_2B_2 monolayers at 300 K (top and side views) at the end of 3 ps AIMD simulations. The Mo, B, and Na atoms are denoted by violet, green, and orange spheres, respectively.

4. The detailed reasons why structures located on the hull are thermodynamically

stable relative to dissociation into other configurations.

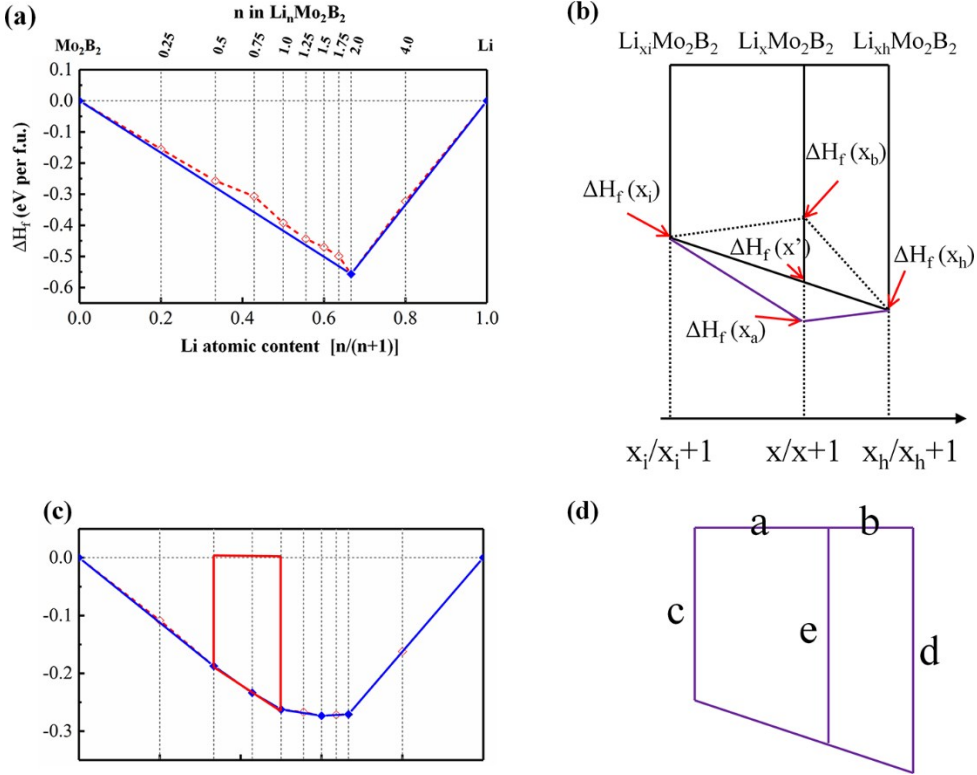
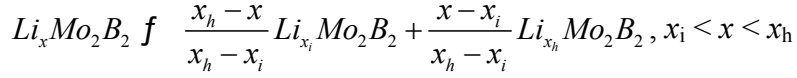


Fig. S15 The convex hull for enthalpies of formation.



$\text{Li}_{x_i}\text{Mo}_2\text{B}_2$ and $\text{Li}_{x_h}\text{Mo}_2\text{B}_2$ are two other configurations for Li adsorption on the 2D Mo_2B_2 . In order to judge the stability of $\text{Li}_x\text{Mo}_2\text{B}_2$, we use the equation as shown below,

$$\Delta E = E(\text{Li}_x\text{Mo}_2\text{B}_2) - \frac{x_h - x}{x_h - x_i} E(\text{Li}_{x_i}\text{Mo}_2\text{B}_2) - \frac{x - x_i}{x_h - x_i} E(\text{Li}_{x_h}\text{Mo}_2\text{B}_2).$$

If $\Delta E > 0$, $\text{Li}_x\text{Mo}_2\text{B}_2$ is unstable and easy to decompose into two other configurations.

If $\Delta E \leq 0$, $\text{Li}_x\text{Mo}_2\text{B}_2$ is stable relative to dissociation into other configurations.

According to Eqn (5), we obtain the following two relations.

$$\text{For } \text{Li}_{x_i}\text{Mo}_2\text{B}_2, \Delta H_f(x_i) = \frac{E(\text{Li}_{x_i}\text{Mo}_2\text{B}_2) - x_i E(\text{Li}) - E(\text{Mo}_2\text{B}_2)}{1 + x_i}.$$

$$\text{For } \text{Li}_{x_h}\text{Mo}_2\text{B}_2, \Delta H_f(x_h) = \frac{E(\text{Li}_{x_h}\text{Mo}_2\text{B}_2) - x_h E(\text{Li}) - E(\text{Mo}_2\text{B}_2)}{1 + x_h}.$$

As shown in Fig. S15d, for a trapezoid, $e = c \times \frac{b}{a+b} + d \times \frac{a}{a+b}$. Then, we can obtain

$\Delta H_f(x')$ from $\Delta H_f(x_i)$, $\Delta H_f(x_h)$, x_i/x_i+1 , x_h/x_h+1 , and $x/x+1$. The equation is given below.

$$\begin{aligned}\Delta H_f(x') &= \frac{\frac{x_h}{x_h+1} - \frac{x}{x+1}}{\frac{x_h}{x_h+1} - \frac{x_i}{x_i+1}} \times \frac{E(Li_{x_i} Mo_2 B_2) - x_i E(Li) - E(Mo_2 B_2)}{1+x_i} + \frac{\frac{x}{x+1} - \frac{x_i}{x_i+1}}{\frac{x_h}{x_h+1} - \frac{x_i}{x_i+1}} \times \frac{E(Li_{x_h} Mo_2 B_2) - x_h E(Li) - E(Mo_2 B_2)}{1+x_h} \\ &= \frac{(x_h - x)(x_i + 1)}{(x_h - x_i)(x + 1)} \times \frac{E(Li_{x_i} Mo_2 B_2) - x_i E(Li) - E(Mo_2 B_2)}{1+x_i} + \frac{(x - x_i)(x_h + 1)}{(x_h - x_i)(x + 1)} \times \frac{E(Li_{x_h} Mo_2 B_2) - x_h E(Li) - E(Mo_2 B_2)}{1+x_h} \\ &= \frac{(x_h - x)}{(x_h - x_i)(x + 1)} \times (E(Li_{x_i} Mo_2 B_2) - x_i E(Li) - E(Mo_2 B_2)) + \frac{(x - x_i)}{(x_h - x_i)(x + 1)} \times (E(Li_{x_h} Mo_2 B_2) - x_h E(Li) - E(Mo_2 B_2)) \\ &= \frac{(x_h - x)}{(x_h - x_i)(x + 1)} \times E(Li_{x_i} Mo_2 B_2) + \frac{(x - x_i)}{(x_h - x_i)(x + 1)} \times E(Li_{x_h} Mo_2 B_2) - \frac{(x_h - x)x_i + (x - x_i)x_h}{(x_h - x_i)(x + 1)} E(Li) - \frac{(x_h - x) + (x - x_i)}{(x_h - x_i)(x + 1)} E(Mo_2 B_2) \\ &= \frac{(x_h - x)}{(x_h - x_i)(x + 1)} \times E(Li_{x_i} Mo_2 B_2) + \frac{(x - x_i)}{(x_h - x_i)(x + 1)} \times E(Li_{x_h} Mo_2 B_2) - \frac{x}{(x + 1)} E(Li) - \frac{1}{(x + 1)} E(Mo_2 B_2)\end{aligned}$$

As shown in Fig. S15b, x_a represents the structure located on the hull, while x_b represents the structure above the hull. It can be found that $\Delta H_f(x_a)$ is smaller than $\Delta H_f(x')$ ($\Delta H_f(x_a) < \Delta H_f(x')$). This is because that $\Delta H_f(x_a)$ is negative and possess a bigger absolute value than $\Delta H_f(x')$. Then, we obtain the following equation.

$$\begin{aligned}\Delta H_f(x_a) - \Delta H_f(x') &= \frac{E(Li_x Mo_2 B_2) - x E(Li) - E(Mo_2 B_2)}{1+x} \\ &- \left(\frac{(x_h - x)}{(x_h - x_i)(x + 1)} \times E(Li_{x_i} Mo_2 B_2) + \frac{(x - x_i)}{(x_h - x_i)(x + 1)} \times E(Li_{x_h} Mo_2 B_2) - \frac{x}{(x + 1)} E(Li) - \frac{1}{(x + 1)} E(Mo_2 B_2) \right) \\ &= \frac{1}{x+1} \left(E(Li_x Mo_2 B_2) - \frac{(x_h - x)}{(x_h - x_i)} \times E(Li_{x_i} Mo_2 B_2) - \frac{(x - x_i)}{(x_h - x_i)} \times E(Li_{x_h} Mo_2 B_2) \right) \\ &= \frac{1}{x+1} \times \Delta E < 0\end{aligned}$$

Thus, $\Delta E < 0$. Therefore, $Li_x Mo_2 B_2$ is thermodynamically stable relative to dissociation into other configurations.

For the structure located above the hull (x_b), $\Delta H_f(x_b)$ is larger than $\Delta H_f(x')$ ($\Delta H_f(x_b) > \Delta H_f(x')$). Then, $\Delta E > 0$. Thus, $Li_x Mo_2 B_2$ is unstable and easy to decompose into other configurations.

